PINK1 Contained in huMSCs-Exosomes Prevents Cardiomyocyte Mitochondrial Calcium Overload in Sepsis by Recovering Mitochondrial Ca^{2+} Efflux

Qin Zhou
Chongqing Medical University Affiliated Children's Hospital
Min Xie
Chongqing Medical University Affiliated Children's Hospital https://orcid.org/0000-0002-8700-2927
Jing Zhu
Chongqing Medical University Affiliated Children's Hospital
Qing Yi
Chongqing Medical University Affiliated Children's Hospital
Bin Tan
Chongqing Medical University Affiliated Children's Hospital
Yasha Li
Chongqing Medical University Affiliated Children's Hospital
Liang Ye
Chongqing Medical University Affiliated Children's Hospital
Xinyuan Zhang
Chongqing Medical University Affiliated Children's Hospital
Ying Zhang
Chongqing Medical University Affiliated Children's Hospital
Jie Tian
Chongqing Medical University Affiliated Children's Hospital
Hao Xu (lb7pl@163.com)
Children's Hospital of Chongqing Medical University

Research

Keywords: sepsis, cardiac dysfunction, PINK1, calcium overload, mitochondrial Ca2+ efflux

Posted Date: November 6th, 2020

DOI: https://doi.org/10.21203/rs.3.rs-100228/v1

Abstract

Background: Sepsis is a systemic inflammatory response to a local severe infection that can lead to multiple organ failure and ultimately death. Studies have shown that 40%-50% of septic patients have diverse myocardial injuries, with mortality ranging from 70% to 90% in contrast to 20% in septic patients without myocardial injury. Therefore, uncovering the mechanism of myocardial injury induced by sepsis and finding a treatment for the corresponding target are immensely important.

Methods: We employed cecal ligation and puncture (CLP) for inducing sepsis in mice, and detect the situation of myocardial injury and cardiac function through serological markers and echocardiography. The cardiomyocytes apoptosis and the ultrastructural of heart tissue detected by TUNEL and transmission electron microscope (TEM) respectively. The Fura-2 AM was used to monitored Ca2+ uptake and efflux of mitochondria. FQ-PCR and Western blot detected the expression of mitochondria Ca2+ distribution regulators and PINK1. JC-1 was used to detected the mitochondrial membrane potential (Δψm) of cardiomyocytes.

Results: We found that the expression of PINK1 decreased in mouse hearts during sepsis, which caused cardiomyocyte mitochondrial calcium efflux disorder, mitochondrial calcium overload and cardiomyocyte injury. In contrast, we found that exosomes isolated from huMSCs (huMSCs-exo) carried Pink1 mRNA that could be transferred to recipient cardiomyocytes, increasing PINK1 expression. Then, the reduction in cardiomyocyte mitochondrial calcium efflux was reversed, and cardiomyocytes recovered from their injury. Furthermore, we confirmed the effect of the PINK1-PKA-NCLX axis on mitochondrial calcium homeostasis in cardiomyocytes during sepsis.

Conclusion: The PINK1-PKA-NCLX axis play an important role in cardiomyocytes mitochondrial calcium efflux, therefore PINK1 could be a therapeutic target to protect cardiomyocyte mitochondria, and the application of huMSCs-exo is a promising strategy against heart dysfunction induced by sepsis.

Introduction

Sepsis is a systemic inflammatory response to a local severe infection that can lead to multiple organ failure and ultimately death, especially in patients with cardiac dysfunction, and mortality increases to 70%-90% compared with patients without cardiac dysfunction[1]. Cardiac injury or dysfunction induced by sepsis subsequently contributes to cardiovascular collapse, resulting in poor perfusion of blood into multiple tissues[2]. Therefore, protecting the heart from injury during sepsis would provide beneficial effects on mortality in this complex disease. In recent years, mesenchymal stem cells (MSCs) have been shown to be effective at reducing mortality and improving myocardial function in animal models of sepsis[3–5]. The MSCs home mainly to the lung and liver after systemic infusion in these models, and few are detected in cardiac tissue[6,7]. Hence, MSC-induced cardiac benefits during sepsis may not be related to their local actions but to their paracrine effects from a distance.

It is known that the beneficial effect of MSCs is mediated by paracrine factors, such as cytokines, growth factors and extracellular vesicles. Exosomes, a type of extracellular vesicle, have been widely reported to mediate local and systemic cell-to-cell communication; they are 30–100 nanometer-sized membrane vesicles and can transfer a specific set of functional RNAs (miRNAs, mRNAs and lncRNAs) and proteins into recipient cells[8]. Several studies have shown that MSCs-exo were able to improve recovery in animal models of liver fibrosis, kidney failure, and myocardial ischemia/reperfusion injury[9–11]. Xiaohong Wang et al. reported that MSCs-exo also contribute to cardioprotective effects in sepsis[11], but how MSCs-exo exert cardioprotective effects during sepsis remains to be elucidated.

Studies have reported that mitochondrial structural abnormalities are observed at the early stage of sepsis, and mitochondrial respiration function is reduced significantly and causes a reduction in ATP production, which leads to myocardial contractility dysfunction[12,13]. The obstruction of mitochondrial Ca^{2+} ($_{m}Ca^{2+}$) efflux mediated by the mitochondrial Na^{+}/Ca^{2+} exchanger (NCLX) is an important mechanism of mitochondrial damage[14], and the activity of NCLX is regulated by PTEN-induced putative kinase 1 (PINK1)[15]. Therefore, in this study, we investigate whether MSCs-exo protect heart function during sepsis by reducing mitochondrial damage and whether MSCs-exo repair mitochondrial damage through PINK1 and NCLX. We believe that this study may provide a novel idea for treating heart dysfunction induced by sepsis and improve the prognosis of sepsis patients.

Methods

Animals and sepsis model

C57BL/6 mice aged 6–8 weeks were obtained from and raised at Chongqing Medical University. CLP was performed to establish a model of sepsis[16]. Briefly, the animals were anesthetized with pentobarbital (1%, 50 mg/kg body weight i.p.), and small scissors were used to make the incision and gain entry into the peritoneal cavity. The cecum was located and exteriorized, after which it was ligated and punctured with a 26-gauge needle at the designated position to induce mid-grade sepsis. The cecum was relocated into the abdominal cavity, and the incision was closed.

Echocardiography

Mice in each group were administered an anesthetic at the corresponding time point after modeling, after which the chest skin was depilated and the mice were placed on a plate to maintain anesthesia and sedation. Transthoracic echocardiography was performed using a high-frequency, high-resolution digital imaging system (Vevo 2100 Imaging System) with a transducer probe (VisualSonics 550D). Thick gel was applied to the chest, the probe was placed on the left edge of the sternum, and two-dimensional B-mode ultrasound was used to display the standard left ventricular short-axis view; then, the probe was moved to the level of the papillary muscles, and M-mode ultrasound was used to record the left ventricular motion curve. All echocardiograms were performed by a single trained individual.

Serological markers of myocardial injury detection

At least 500 μL of whole blood per mouse was saved in heparin, and the plasma was collected after centrifugation at 8000 rpm for 10 min. The levels of α-hydroxybutyrate dehydrogenase(HBDH) and creatine kinase (CK) in plasma were measured by an automatic biochemical analyzer (C701, Roche, Switzerland). Cardiac troponin-I (cTnI) was quantified by ELISA (E-EL-M1203c, Elabscience, China).

Cell culture and treatments

The huMSCs used in our study were obtained from Chongqing Stem Cell Therapy Engineering and Technology Center and cultured in DMEM/F12 supplemented with 10% fetal bovine serum (FBS; Millipore, USA). Adult mouse cardiomyocytes (ACMs) were isolated from adult mouse hearts and cultured in dishes or plates precoated with mouse laminin17. Human ventricular myocyte AC16 cells were cultured in DMEM supplemented with 10% fetal bovine serum and treated with LPS (5 μg/ml) to build an in vitro sepsis model. Then, AC16 cells were treated with forskolin (20 μM, 12 hr) or the protein kinase A (PKA) inhibitor H89 (5 μM, 12 hr).

Transient transfection with siRNA

The huMSCs were transfected with siRNA according to the manufacturer's instructions. Transfection of siRNA into huMSCs was performed utilizing RNAiMax reagent (Thermo Fisher Scientific, USA) at a final concentration of 100 nM. Cellular RNA and culture medium supernatant collection was conducted 48 hr after transfection. The siRNA sequence for *Pink1* was 5'-GGCTGGTGATCGCAGATTT-3'

Isolation and characterization of exosomes

Twenty-four hours before the collection of exosomes from huMSCs and huMSCs transfected with *Pink1* siRNA, the medium was replaced with medium containing 10% exosome-depleted FBS. Supernatants were collected and centrifuged successively at 300 × g for 10 min, 2000 × g for 10 min and 10000 × g for 30 min, and at each step, the supernatants were transferred to a new tube. The final supernatant was then ultracentrifuged at 100000 × g for 70 min, and the pellet was washed in PBS and ultracentrifuged at 100000 × g for 70 min once more[18]. Finally, the pellet was resuspended in PBS and quantified by BCA assay. Then, the mice were treated with exosomes at 2 μg/g and cocultured with cells at 2 μg/ml. The quality of the exosomes was confirmed by transmission electron microscopy, particle size assessment (ZEN3600, Malvern, United Kingdom) and exosome markers.

Fluorescence quantitative PCR

Total RNA was isolated from rat hearts using TRIzol (Takara, Japan) according to the instructions. cDNA was generated using 1 μg RNA with a PrimeScriptTM RT Reagent Kit (Takara, Japan). FQ-PCR was performed using TB Green (Takara, Japan) with a CFX-96 (BIO-RAD, USA). We evaluated samples for mRNA expression of *Mcu*, *Micu1*, *Nclx* and *Pink1*. All experimental samples were analyzed in triplicate and averaged. To calculate the fold change in mRNA expression, the $2^{-\Delta\Delta Ct}$ method was used.

Western blotting

Proteins were isolated from rat hearts using lysis buffer (KeyGEN BioTECH, China) with protease and phosphatase inhibitor cocktail solution (KeyGEN BioTECH, China). Thirty micrograms of protein was loaded on a 10% PAGE Gel Fast Preparation Kit (PG112, Epizyme Biotech, China). After Western blotting was performed, PVDF membranes (Millipore, USA) were incubated in TBST skimmed milk blocking buffer for 1 hr at RT and then with primary antibodies overnight at 4°C. Primary antibodies against the following were used: CD81 (sc-166029, Santa Cruz, USA), Alix (sc-53540, Santa Cruz, USA), MCU (26312-1-AP, Proteintech, USA), MICU1 (ab224161, Abcam, England), NCLX (ab83551, Abcam, England), PINK1 (23274-1-AP, Proteintech, USA), and GAPDH (AF7021, Affinity Biosciences, USA). After washing with TBST three times, the membranes were incubated with secondary antibodies (701051, Zen Bioscience, China; ZB-2301, ZSGB-BIO, China) for 1 hr at RT and washed with TBST three times again. Membranes were probed with a chemiluminescence kit (Millipore, USA) using an Image system (Bio-Rad, USA).

TUNEL

The tissue was fixed in 4% paraformaldehyde for at least 24 hr, embedded in paraffin and sectioned into 4 μm slices. Then, apoptosis was assessed using a TUNEL kit (KGA702-1, KeyGEN BioTECH, China) according to the manufacturer's instructions. Images were acquired on a Nikon microscope (90i, Japan).

TEM

Heart tissue was fixed with 4% glutaraldehyde solution for 2 hr and then postfixed with 1% osmium tetroxide for 2 hr at 4°C. The fixed tissue was rinsed with distilled water, dehydrated with an ethanol and methanol gradient, and

embedded in epoxy resin. Subsequently, the samples were sectioned and contrast-stained for imaging. TEM images were acquired at random locations throughout the samples. Micrographs were taken with a TEM (TEM; H-7500).

Evaluation of $_{m}Ca^{2+}$ uptake and efflux

ACMs or AC16 (300000) were transferred to an intracellular-like medium containing 120 mM KCl, 10 mM NaCl, 1 mM KH_2PO_4, 20 mM HEPES-Tris, 3 mM thapsigargin, 80 μg ml^{-1} digitonin, protease inhibitors, and 10 μM succinate at pH 7.2. Fura-2 AM (1 μM) was added to monitor extramitochondrial Ca^{2+}. Fluorescence signals were monitored at excitations of 340 and 380 nm and an emission of 510 nm for Fura-2 to calculate ratiometric changes. At 60 s, a 20 μM Ca^{2+} bolus was added. Clearance of extramitochondrial Ca^{2+} was representative of $_{m}Ca^{2+}$ uptake. At 260 s, 1 μM Ru360 (MCU-inhibitor) was added to inhibit uptake and allow for quantification of $_{m}Ca^{2+}$ efflux. At 360 s, 10 μM CGP-37157 (NCLX inhibitor) was added to block $_{m}Ca^{2+}$ efflux. At completion of the experiment, FCCP was added. All experiments were conducted at 37°C and recorded on a Cytation 5 (Biotek, USA); the details have been previously reported[14].

Mitochondrial membrane potential assay

The mitochondrial membrane potential was measured using a mitochondrial membrane potential assay kit (JC-1, Beyotime Biotech, China) according to the manufacturer's instructions. Cells were incubated with medium mixed with JC-1 working fluid in a 37℃ incubator for 20 min. Then, the cells were washed with JC-1 buffer three times and replaced with fresh medium. Finally, the fluorescence was captured by confocal microscopy (A1R, Nikon, Japan). The ratio of red and green fluorescence was analyzed by an NIS-Elements system (Nikon, Japan). A high ratio indicates a high mitochondrial membrane potential.

Statistical analysis

Each experiment was repeated at least three times. All data are expressed as the means ± SD, while the statistical evaluations were performed using t-tests with independent samples, continuity correction chi-square tests and one-way ANOVA. SPSS 17.0 software (SPSS Inc., Armonk, NY, USA) was used for the statistical analysis. For all analyses, a value of $P<0.05$ was considered to be significant.

Results

huMSCs-exo showed cardioprotective effects in a sepsis model

huMSCs-exo were isolated and purified through differential ultracentrifugation, after which they were assess by TEM, exosome markers and particle size (Fig 1. A-C). We employed CLP to investigate the cardioprotective effects of huMSCs-exo in septic mice. A 2 μg/g concentration of huMSCs-exo was intraperitoneally injected at 0 hr and 6 hr after CLP, followed by testing at 12 hr after CLP. We found that the serum markers of cardiomyocyte injury (HBDH, CK and cTnI) increased significantly after CLP, which indicates that sepsis could induce cardiomyocyte injury in the first 12 hr. In contrast, these markers decreased markedly in the huMSCs-exo treatment group (Fig 1. D), which indicates that treatment with huMSCs-exo could effectively mitigate cardiomyocyte injury induced by sepsis. Next, we used the ejection fraction (EF), measured by echocardiography, to reflect heart function during sepsis. The results showed that EF decreased notably at 12 hr after CLP and that huMSCs-exo significantly improved EF in contrast with the CLP group (Fig 1. E, F), which indicated that huMSCs-exo could prevent heart function disorder induced by sepsis. In addition, we found that after huMSCs-exo treatment, CLP mouse survival significantly increased compared with the

untreated group (Fig 1. G). Hence, we hypothesized that the increase in the mouse survival rate in the treatment group was highly correlated with heart function, which was protected by huMSCs-exo during sepsis.

huMSCs-exo protected cardiomyocyte mitochondria from damage induced by sepsis

To investigate the extent of cardiomyocyte injury in early sepsis, we used TUNEL to check cardiomyocyte apoptosis. We found that even though serum markers of cardiomyocyte injury increased significantly, there was almost no apoptosis in cardiomyocytes at 12 hr after CLP, and some cardiomyocytes did not undergo apoptosis until 24 hr after CLP (Fig 2. A). This suggests that at 12 hr of sepsis, cardiomyocytes were in the early stage of apoptosis, and some factors increased cardiomyocyte membrane permeability and resulted in cardiac-specific protein release.

To reveal the reason for increased injury markers and to find changes in cardiomyocytes during the first 12 hr of sepsis, we observed cardiomyocyte ultrastructure by TEM. We observed a disorderly myocardial myofibril arrangement, and that the band area was blurred, broken or dissolved at 12 hr after CLP, although cardiomyocyte apoptosis did not occur at this time. Furthermore, we also observed that cardiomyocyte mitochondrial swelling, cristae disorganization and cristae number decreased, which indicated that cardiomyocyte mitochondria were seriously injured during the first 12 hr of sepsis (Fig 2. B). Mitochondrial dysfunction is one of the most important pathways that induces cell apoptosis; therefore, mitochondrial injury is an upstream event of cardiomyocyte apoptosis in sepsis. One of the main characteristics of mitochondrial dysfunction is reduced ATP production, which matched our results, and we found that ATP production was significantly reduced at 12 hr after CLP (Fig 2. C).

We wondered whether the cardioprotective effects of huMSCs-exo were exerted through mitochondria protection. Therefore, we checked the cardiomyocytes' ultrastructure by TEM after treatment with huMSCs-exo and found that myocardial myofibrils were arranged in order and that no broken or dissolved myofibrils were observed; in addition, the mitochondria morphology was nearly as normal as the sham group, with only a few mitochondria showing a decrease in the number of cristae (Fig 2. B). This observation indicates that huMSCs-exo could effectively prevent cardiomyocyte mitochondrial injury in the first 12 hr of sepsis. Furthermore, the ATP production of cardiomyocytes in the treatment group at 12 hr after CLP was increased, which was close to the level of the sham group (Fig 2. C), which might be a benefit from undamaged mitochondria protected by huMSCs-exo. According to these results, we hypothesized that huMSCs-exo could protect cardiomyocytes from damage induced by sepsis by preventing mitochondrial injury in the early stage of sepsis to subsequently reduce cardiomyocyte apoptosis.

Cardiomyocyte mitochondrial Ca^{2+} ($_mCa^{2+}$) efflux was obstructed during sepsis and reversed by huMSCs-exo

One study reported that in the early stage of sepsis, Ca^{2+} overinflows into the cytoplasm from the extracellular space of cardiomyocytes, and mitochondrial uptake overloads Ca^{2+} in the matrix, which ultimately induces mitochondrial calcium overload. Cardiomyocyte injury induced by mitochondrial calcium overload is an important mechanism that causes heart dysfunction in sepsis. To investigate how mitochondrial calcium overload of cardiomyocytes occurs in sepsis, we assessed the capacity of Ca^{2+} uptake and efflux in cardiomyocyte mitochondria. Adult cardiomyocytes (ACMs) isolated from sham-, CLP- and huMSCs-exo-treated mice were transferred to an intracellular-like medium, after which 1 μM Fura2-AM was added to monitor extramitochondrial Ca^{2+} and thapsigargin was added to prevent SR and ER Ca^{2+} uptake; hence, the changes in the fluorescence intensity indicated Ca^{2+} influx or efflux into/out of the mitochondria. The results showed that after the Ca^{2+} bolus was added, the time for extra-mitochondrial Ca^{2+} to reach the low point occurred earlier in the CLP group than in the sham group (Fig 3. A, B 60 s-260 s), which indicated that mitochondrial Ca^{2+} uptake in the CLP group was slightly faster than that in the sham group. After MCU was inhibited by Ru360 at 260 s-360 s, Ca^{2+} uptake in the mitochondria was blocked, and the increase in extramitochondrial Ca^{2+}

was representative of $_{m}Ca^{2+}$ efflux. The results showed that during the same period of time, the peak of extramitochondrial Ca^{2+} reached in the CLP group was much lower than that in the sham group (Fig 3. A, B 260 s-360 s, D), which indicates that the $_{m}Ca^{2+}$ efflux rate decreased significantly in the CLP group. In contrast, we found that although Ca^{2+} uptake by mitochondria in the huMSCs-exo treatment group was not different from that in the CLP group (Fig 3. C 60 s-260 s), the $_{m}Ca^{2+}$ efflux rate increased to the level of the sham group (Fig 3. C 260 s-360 s, D), suggesting that huMSCs-exo could keep the $_{m}Ca^{2+}$ efflux of cardiomyocyte mitochondria normal during sepsis. According to these results, we hypothesize that abnormal cardiomyocyte $_{m}Ca^{2+}$ efflux is an important reason for cardiomyocyte mitochondrial calcium overload, which causes mitochondrial dysfunction and finally induces cardiomyocyte apoptosis; furthermore, huMSCs-exo may protect heart function during sepsis by avoiding mitochondrial calcium overload induced by abnormal $_{m}Ca^{2+}$ efflux.

Mitochondria regulate $_{m}Ca^{2+}$ distribution in two ways: cytoplasmic Ca^{2+} uptake is driven by ΔΨm and mediated mainly by MCU and MICU1[19], and $_{m}Ca^{2+}$ efflux is mediated by mitochondrial NCLX[20]. We assessed the expression of MCU, MICU1 and NCLX 12 hr after CLP, and there was little difference between the sham and CLP groups (Fig 3. E, F). This result indicates that the expression of these $_{m}Ca^{2+}$ distribution regulators in cardiomyocytes was not affected during sepsis; therefore, in our opinion, the reason for abnormal $_{m}Ca^{2+}$ efflux at 12 hr after CLP may be that the activity of NCLX was depressed.

huMSCs-exo increased the expression of PINK1 in cardiomyocytes during sepsis

Studies have indicated that the activity of NCLX is regulated by several proteins and kinases, such as stomatin-like protein 2 (SLP-2) and protein kinase C (PKC)[21,22]. Research has shown that in a cell model of Parkinson's disease related to mutations in PINK1, the failure of mitochondrial Ca^{2+} efflux in neurons deficient in PINK1 is linked to the impaired activity of NCLX, which results in mitochondrial Ca^{2+} overload[15,23]. Therefore, we wondered whether PINK1 also regulated the activity of NCLX in cardiomyocytes. We found that at 12 hr after CLP, the expression of PINK1 decreased significantly (Fig 4. A), which matched the result that $_{m}Ca^{2+}$ efflux was abnormal, suggesting that in cardiomyocytes, the decrease in PINK1 expression may be associated with a reduction in NCLX activity.

In addition, we found that after huMSCs-exo treatment, in addition to $_{m}Ca^{2+}$ efflux being unaffected, PINK1 expression also increased in septic mouse cardiomyocytes (Fig 4. A), further confirming the relationship between PINK1 expression and NCLX activity. To further explore the source of increased PINK1 in cardiomyocytes after huMSCs-exo treatment, we detected *Pink1* mRNA in huMSCs and their exosomes and found that huMSCs-exo carried more *Pink1* mRNA than in the huMSCs (Fig 4. B). We hypothesized that this result indicates that in addition to meeting the physiological needs of huMSCs, *Pink1* tended to be contained in exosomes and secreted extracellularly, which were used to regulate *Pink1* expression in recipient cells.

We next used *Pink1*-specific siRNA to inhibit *Pink1* expression in huMSCs to confirm whether huMSCs-exo increased PINK1 expression in recipient cardiomyocytes by transferring *Pink1* mRNA from huMSCs. *Pink1* expression was dramatically inhibited by *Pink1* siRNA in both huMSCs and their exosomes (Fig 4. C), and PINK1 expression in ACMs isolated from mice treated with *Pink1*-inhibited huMSCs exosomes was still at a low level (Fig 4. D), suggesting that the increased PINK1 expression in recipient cardiomyocytes comes from *Pink1* mRNA carried in huMSCs-exo.

huMSCs-exo with inhibited *Pink1* could not reverse $_{m}Ca^{2+}$ efflux obstruction and mitochondrial damage induced by sepsis

To further validate that PINK1 is related to NCLX-mediated $_{m}Ca^{2+}$ efflux, we monitored the $_{m}Ca^{2+}$ efflux rate of ACMs from mice treated with *Pink1*-inhibited huMSCs-exo. In our results, no significant difference was detected between the CLP and CLP treated with exo$^{pink1\ siRNA}$ groups (Fig 5. B, D, E). In contrast, the $_{m}Ca^{2+}$ efflux rate in the CLP treated with exo$^{Neg\ siRNA}$ group was the same as that of the sham group (Fig 5. A, C, E). This suggests that the loss of *Pink1* mRNA attenuated the ability of huMSCs-exo to recover $_{m}Ca^{2+}$ efflux. Then, whether this loss also weakened the ability of huMSCs-exo to keep mitochondria from sepsis-induced damage remains unclear. We observed mitochondrial morphology with TEM and found that the mitochondrial cristae number still decreased and the arrangement was disordered in CLP mice with exo$^{pink1\ siRNA}$ treatment (Fig5. F). This indicates that mitochondrial protection of huMSCs-exo was greatly weakened after *Pink1* mRNA inhibition. We confirmed from these results that PINK1 was important for the regulation of NCLX-mediated $_{m}Ca^{2+}$ efflux, that cardiomyocyte $_{m}Ca^{2+}$ efflux obstruction during sepsis was a crucial reason for mitochondrial damage, and that *Pink1* mRNA contained in huMSCs-exo was a central factor that reversed $_{m}Ca^{2+}$ efflux obstruction induced by sepsis to prevent mitochondrial damage.

PINK1 regulated NCLX-mediated $_{m}Ca^{2+}$ efflux possibly by affecting PKA activity after transfer from huMSCs-exo to cardiomyocytes

The above results have confirmed the effect of PINK1 on NCLX-mediated $_{m}Ca^{2+}$ efflux, but no evidence has shown that the interaction between PINK1 and NCLX is direct. In contrast, many studies argue against a direct interaction of PINK1 and NCLX. These studies have indicated that bioinformatic analysis failed to identify any PINK1 phosphorylation site on NCLX and that proteomic analysis of PINK1-interacting proteins found 14 candidates but not NCLX[15,24]. After transfer from huMSCs-exo to the cardiomyocytes, the pathway by which PINK1 regulates NCLX-mediated $_{m}Ca^{2+}$ efflux is unknown. One study showed that PINK1-deficient cells exhibit PKA inhibition and NCLX-mediated $_{m}Ca^{2+}$ efflux impairment, which could be fully rescued by activated PKA.

To determine whether PINK1 regulated NCLX-mediated $_{m}Ca^{2+}$ efflux through PKA, we used forskolin (FSK) and H89 to activate and inhibit PKA, respectively. AC16 cells were treated with LPS and huMSCs-exo, after which we monitored the $_{m}Ca^{2+}$ efflux rate. The results showed that PKA activation by FSK (Fig 6. A, B light green) could enhance the $_{m}Ca^{2+}$ efflux rate compared with treatment with huMSCs-exo alone (Fig 6. A, B blue). In addition, consistent with a previous study[15], we found that FSK greatly recovered the $_{m}Ca^{2+}$ efflux rate decrease caused by the absence of PINK1 (Fig 6. C, D, gray and green) and that the ΔΨm also increased (Fig 6. E, G). However, coapplication of FSK and H89 completely abolished $_{m}Ca^{2+}$ efflux activation (Fig 6. A, B light orange; C, D orange) and inhibited the increasing ΔΨm (Fig 6. E, F, G) both in the huMSCs-exo and huMSCs-exo$^{pink1\ siRNA}$ treatment groups. These results suggest that PKA is essential for PINK1-regulated NCLX-mediated $_{m}Ca^{2+}$ efflux.

Discussion

The heart is an important target organ in severe sepsis/septic shock, and its dysfunction can manifest in multiple different ways in sepsis, including left and/or right ventricular impairment during systole or diastole, inadequate cardiac output and oxygen delivery, or primary myocardial cellular injury[25]. Sepsis with cardiac dysfunction can increase mortality by 50%, which should arouse our attention. At present, fluid resuscitation is used clinically to improve cardiac perfusion, cardiac output and systolic function at the early stage of sepsis to support the heart, but there is no specific treatment. This is probably because of the unclear and complicated mechanism of sepsis-induced cardiac dysfunction, which explains the lack of drugs aimed at corresponding targets. Previous studies have

indicated that the main proposed mechanisms underlying the pathophysiology of myocardial dysfunction in sepsis support a prominent role for functional rather than anatomical abnormalities[26]. Clinically significant pathophysiological changes in cardiac function taking place early during sepsis can occur in the absence of cellular hypoxia or histologic changes, suggesting that severe metabolic derangement might underlie the development of septic cardiomyopathy[27–30]. This opinion is consistent with our results in this study, which showed cardiomyocyte mitochondrial damage much earlier than cardiomyocyte apoptosis. Mitochondrial damage is an important trigger that causes apoptosis, which is characterized by a change in mitochondrial architecture (swelling, internal vesicle formation, and abnormalities in cristae), mitochondrial DNA damage and elevation in mitochondrial permeability transition[13,31,32]. Mitochondria, as power houses, provide continuous energy for heart activity, and injury inevitably induces metabolic derangement and eventually causes heart dysfunction. Therefore, mitochondria could be a promising target treatment against heart dysfunction induced by sepsis and improve the prognosis of sepsis patients.

We found that exosomes secreted from huMSCs could extenuate cardiomyocyte injury induced by sepsis, which is consistent with a previous study[11]. The difference in our study is that we confirmed that this extenuation was achieved by repairing the mitochondria. Before exploring the mechanism by which huMSCs-exo repair cardiomyocyte mitochondria, we must first clarify the mechanism of mitochondrial dysfunction induced by sepsis. The reported mechanisms of cardiomyocyte mitochondrial dysfunction induced by sepsis include energy metabolism disorder, calcium overload, autophagy, and mitochondrial inner membrane damage. Calcium acts as an important intracellular second messenger, playing a key role in cardiac contractility. Mitochondria are one of the largest calcium pools in cardiomyocytes and can alleviate the high concentration of Ca^{2+} through uptake of intracellular Ca^{2+} ($_{i}Ca^{2+}$) into the mitochondrial matrix. However, when $_{m}Ca^{2+}$ exceeds the concentration that mitochondria can handle, the mitochondrial permeability transition pore (MPTP) irreversibly open, and the ΔΨm is reduced, which induces mitochondrial dysfunction[33]. Normal mitochondria need ΔΨm to maintain their function, and a decreased ΔΨm is an important cause of apoptosis. It has been confirmed that calcium overload is an upstream event of mitochondrial depolarization[15]. Therefore, mitochondrial calcium overload may be an important mechanism of mitochondrial dysfunction in septic hearts. This view is further confirmed in this study, in which we found cardiomyocyte impairment of $_{m}Ca^{2+}$ shuttling at 12 hr after CLP, much earlier than apoptosis.

There are two processes that cause mitochondrial calcium overload: excessive calcium uptake into mitochondria that is mainly driven by MCU or a decrease in calcium efflux from the mitochondrial matrix to the cytoplasm. The most important regulator of mitochondrial calcium efflux is NCLX, which is proposed to be the primary mechanism for $_{m}Ca^{2+}$ extrusion in excitable cells[14]. Either abnormal MCU or NCLX can cause $_{m}Ca^{2+}$ shuttling system disorder, but research has shown that an MCU knockout yielded a relatively mild phenotype, while a conditional knockout of NCLX led to rapid fatal heart failure[20], which suggests that NCLX-mediated efflux is necessary to maintain homeostatic $_{m}Ca^{2+}$ levels in cardiomyocytes and is necessary for survival. We found no change in Ca^{2+} uptake by cardiomyocyte mitochondria in the early stage of sepsis, but $_{m}Ca^{2+}$ efflux was obviously abnormal. This suggests that sepsis-induced cardiac dysfunction may be caused by mitochondrial calcium overload resulting from reducing mitochondrial calcium efflux. At the same time, we found that huMSCs-exo could reverse the reduction in cardiomyocyte $_{m}Ca^{2+}$ efflux induced by sepsis, and we believe this may be the way huMSCs-exo exert their cardiac protective function. Exosomes contain multiple kinds of cell-specific proteins, lipids, and nucleic acids, and it is not known which factor in huMSCs is linked to the reversion of $_{m}Ca^{2+}$ efflux reduction.

In contrast, we found that the expression of PINK1, a key protein associated with NCLX-mediated $_{m}Ca^{2+}$ efflux, decreased significantly in CLP mouse hearts. PINK1 is a serine/threonine kinase that was initially linked to the pathogenesis of a familial form of Parkinson's disease[34,35], and its loss-of-function mutations cause dopaminergic neuron mitochondrial calcium overload, which makes cells particularly vulnerable to injury[23]. PINK1 KO mice developed left ventricular dysfunction and cardiac hypertrophy, leading to pressure overload-induced heart failure. In addition, mitochondria from PINK1 KO hearts display an altered morphology, reduced mitochondrial membrane potential and decreased oxidative phosphorylation, which in turn induces oxidative stress and increases cardiomyocyte apoptosis[34,36,37]. Interestingly, we found that huMSCs-exo carried more *Pink1* mRNA than the huMSCs themselves. Furthermore, we showed that *Pink1* mRNA could be transferred from huMSCs-exo into recipient cardiomyocytes after treatment with huMSCs-exo and increase their PINK1 expression. When *Pink1* mRNA contained in huMSCs-exo was inhibited, huMSCs-exo lost the ability of $_{m}Ca^{2+}$ efflux regulation. Therefore, we believe that huMSCs-exo reverse the reduction in cardiomyocyte $_{m}Ca^{2+}$ efflux induced by sepsis by transferring *Pink1* mRNA into cardiomyocytes to restore PINK1 expression.

Although PINK1 is associated with NCLX-mediated $_{m}Ca^{2+}$ efflux, the interaction between PINK1 and NCLX is indirect[24]. In addition, researchers have proven that the loss of PINK1 leads to PKA inhibition and that modulation of the NCLX phosphorylation site by PKA activation is essential for NCLX activity[15,38]. In this study, we found that activated PKA could rescue the LPS-induced reduction in $_{m}Ca^{2+}$ efflux and $\Delta\Psi m$ when huMSCs-exo lost their ability to regulate $_{m}Ca^{2+}$ efflux. This suggests that $_{m}Ca^{2+}$ efflux could be regulated by the PINK1-PKA-NCLX axis in cardiomyocytes, similar to that in neurons, and that sepsis-induced heart dysfunction could be caused by this axis abnormality. Then, we wanted to know whether huMSCs-exo protected cardiomyocytes during sepsis only by upregulating PINK1 expression to rescue the PINK1-PKA-NCLX axis or whether other mechanisms dependent on PINK1 were involved. Research on PINK1 has revealed that its multiple functions extend well beyond mitochondrial calcium efflux regulation. PINK1 has been identified as a crucial player in the mitochondrial quality control pathway[34,39] and promotes damaged mitochondria elimination through Parkin-dependent[40,41] or Parkin-independent[34,42] mitophagy. Therefore, we speculate that after huMSCs-exo increase PINK1 expression in septic cardiomyocytes, PINK1 may eliminate the damaged mitochondria caused by mitochondrial calcium overload by activating mitophagy to protect cardiomyocytes. This hypothesis was not proven in this study, but it enlightens us in the direction of further research.

In conclusion, we first confirmed that sepsis-induced PINK1-PKA-NCLX axis abnormalities in cardiomyocytes were the main cause of cardiomyocyte mitochondrial calcium overload and heart dysfunction. In addition, we found that exosomes secreted from huMSCs could transfer *Pink1* mRNA to cardiomyocytes and rescue the decreased $_{m}Ca^{2+}$ efflux-induced mitochondrial calcium overload by restoring the PINK1-PKA-NCLX axis. The important limitation of this study is that we failed to explore whether PINK1-dependent mitophagy is involved in the cardioprotective effects of huMSCs-exo. In spite of this, our data still support that PINK1 could be a therapeutic target to protect cardiomyocyte mitochondria and that the application of huMSCs-exo is a promising strategy against heart dysfunction induced by sepsis.

Abbreviations

CLP cecal ligation and puncture

TEM transmission electron microscope

Δψm mitochondrial membrane potential

huMSCs-exo exosomes isolated from huMSCs

MSCs mesenchymal stem cells

NCLX mitochondrial Na^+/Ca^{2+} exchanger

PINK1 PTEN-induced putative kinase 1

HBDH α-hydroxybutyrate dehydrogenase

CK creatine kinase

cTnI Cardiac troponin-I

FBS fetal bovine serum

PKA protein kinase A

EF ejection fraction

ACMs Adult cardiomyocytes

SLP-2 stomatin-like protein 2

PKC protein kinase C

FSK forskolin

MPTP mitochondrial permeability transition pore

Declarations

Acknowledgements

We appreciate our colleagues for their valuable efforts on this paper.

Author contributions statement

Hao Xu, Jing Zhu and Jie Tian conceived and designed the project. Qin Zhou, Min Xie and Hao Xu carried out the experiments and drafted the manuscript, Bin Tan contributed to edit the figures. Qin Yi performed statistical analyses. Liang Ye and Yasha Li carried out the sample collection. Yin Zhang and Xinyuan Zhang contributed to cells culture, reagent procurement and management.

Funding

This work was supported by the National Natural Science Foundation of China (Grant Number 81700250 & Grant Number 81670270). We thank department of pediatric research institute for their technical assistance.

Availability of data and materials

The data that support the findings of this study are available from the corresponding author upon reasonable request.

Ethics approval and consent to participate

The current study was approved by the Ethics Committee of the ChongQing Medical University.

Consent for publication

Not applicable.

Competing interests

The authors declare that there are no competing interests associated with the manuscript.

References

1. Zanotti-Cavazzoni SL, Hollenberg SM. Cardiac dysfunction in severe sepsis and septic shock. *Curr Opin Crit Care.* 2009;15(5):392-397.
2. Romero-Bermejo FJ, Ruiz-Bailen M, Gil-Cebrian J, Huertos-Ranchal MJ. Sepsis-induced cardiomyopathy. *Curr Cardiol Rev.* 2011;7(3):163-183.
3. Kusadasi N, Groeneveld AB. A perspective on mesenchymal stromal cell transplantation in the treatment of sepsis. *Shock.* 2013;40(5):352-357.
4. Nemeth K, Leelahavanichkul A, Yuen PS, et al. Bone marrow stromal cells attenuate sepsis via prostaglandin E(2)-dependent reprogramming of host macrophages to increase their interleukin-10 production. *Nat Med.* 2009;15(1):42-49.
5. Anderson P, Souza-Moreira L, Morell M, et al. Adipose-derived mesenchymal stromal cells induce immunomodulatory macrophages which protect from experimental colitis and sepsis. *Gut.* 2013;62(8):1131-1141.
6. Krasnodembskaya A, Samarani G, Song Y, et al. Human mesenchymal stem cells reduce mortality and bacteremia in gram-negative sepsis in mice in part by enhancing the phagocytic activity of blood monocytes. *Am J Physiol Lung Cell Mol Physiol.* 2012;302(10):L1003-1013.
7. Weil BR, Herrmann JL, Abarbanell AM, Manukyan MC, Poynter JA, Meldrum DR. Intravenous infusion of mesenchymal stem cells is associated with improved myocardial function during endotoxemia. *Shock.* 2011;36(3):235-241.
8. Ailawadi S, Wang X, Gu H, Fan GC. Pathologic function and therapeutic potential of exosomes in cardiovascular disease. *Biochim Biophys Acta.* 2015;1852(1):1-11.
9. Li T, Yan Y, Wang B, et al. Exosomes derived from human umbilical cord mesenchymal stem cells alleviate liver fibrosis. *Stem Cells Dev.* 2013;22(6):845-854.
10. Xin H, Li Y, Liu Z, et al. MiR-133b promotes neural plasticity and functional recovery after treatment of stroke with multipotent mesenchymal stromal cells in rats via transfer of exosome-enriched extracellular particles. *Stem Cells.* 2013;31(12):2737-2746.
11. Wang X, Gu H, Qin D, et al. Exosomal miR-223 Contributes to Mesenchymal Stem Cell-Elicited Cardioprotection in Polymicrobial Sepsis. *Sci Rep.* 2015;5:13721.
12. Coalson JJ, Hinshaw LB, Guenter CA, Berrell EL, Greenfield LJ. Pathophysiologic responses of the subhuman primate in experimental septic shock. *Lab Invest.* 1975;32(4):561-569.

13. Martin L, Derwall M, Al Zoubi S, et al. The Septic Heart: Current Understanding of Molecular Mechanisms and Clinical Implications. *Chest.* 2019;155(2):427-437.
14. Luongo TS, Lambert JP, Gross P, et al. The mitochondrial Na(+)/Ca(2+) exchanger is essential for Ca(2+) homeostasis and viability. *Nature.* 2017;545(7652):93-97.
15. Kostic M, Ludtmann MH, Bading H, et al. PKA Phosphorylation of NCLX Reverses Mitochondrial Calcium Overload and Depolarization, Promoting Survival of PINK1-Deficient Dopaminergic Neurons. *Cell Rep.* 2015;13(2):376-386.
16. Rittirsch D, Huber-Lang MS, Flierl MA, Ward PA. Immunodesign of experimental sepsis by cecal ligation and puncture. *Nat Protoc.* 2009;4(1):31-36.
17. Ackers-Johnson M, Foo RS. Langendorff-Free Isolation and Propagation of Adult Mouse Cardiomyocytes. *Methods Mol Biol.* 2019;1940:193-204.
18. Thery C, Amigorena S, Raposo G, Clayton A. Isolation and characterization of exosomes from cell culture supernatants and biological fluids. *Curr Protoc Cell Biol.* 2006;Chapter 3:Unit 3 22.
19. Mallilankaraman K, Doonan P, Cardenas C, et al. MICU1 is an essential gatekeeper for MCU-mediated mitochondrial Ca(2+) uptake that regulates cell survival. *Cell.* 2012;151(3):630-644.
20. Kostic M, Sekler I. Functional properties and mode of regulation of the mitochondrial Na(+)/Ca(2+) exchanger, NCLX. *Semin Cell Dev Biol.* 2019;94:59-65.
21. Da Cruz S, De Marchi U, Frieden M, Parone PA, Martinou JC, Demaurex N. SLP-2 negatively modulates mitochondrial sodium-calcium exchange. *Cell Calcium.* 2010;47(1):11-18.
22. Yang F, He XP, Russell J, Lu B. Ca2+ influx-independent synaptic potentiation mediated by mitochondrial Na(+)-Ca2+ exchanger and protein kinase C. *J Cell Biol.* 2003;163(3):511-523.
23. Gandhi S, Wood-Kaczmar A, Yao Z, et al. PINK1-associated Parkinson's disease is caused by neuronal vulnerability to calcium-induced cell death. *Mol Cell.* 2009;33(5):627-638.
24. Rakovic A, Grunewald A, Voges L, et al. PINK1-Interacting Proteins: Proteomic Analysis of Overexpressed PINK1. *Parkinsons Dis.* 2011;2011:153979.
25. Beesley SJ, Weber G, Sarge T, et al. Septic Cardiomyopathy. *Crit Care Med.* 2018;46(4):625-634.
26. Celes MR, Prado CM, Rossi MA. Sepsis: going to the heart of the matter. *Pathobiology.* 2013;80(2):70-86.
27. dos Santos CC, Gattas DJ, Tsoporis JN, et al. Sepsis-induced myocardial depression is associated with transcriptional changes in energy metabolism and contractile related genes: a physiological and gene expression-based approach. *Crit Care Med.* 2010;38(3):894-902.
28. Finkel MS, Oddis CV, Jacob TD, Watkins SC, Hattler BG, Simmons RL. Negative inotropic effects of cytokines on the heart mediated by nitric oxide. *Science.* 1992;257(5068):387-389.
29. Hotchkiss RS, Karl IE. Reevaluation of the role of cellular hypoxia and bioenergetic failure in sepsis. *JAMA.* 1992;267(11):1503-1510.
30. Piper RD, Li FY, Myers ML, Sibbald WJ. Structure-function relationships in the septic rat heart. *Am J Respir Crit Care Med.* 1997;156(5):1473-1482.
31. Suliman HB, Carraway MS, Piantadosi CA. Postlipopolysaccharide oxidative damage of mitochondrial DNA. *Am J Respir Crit Care Med.* 2003;167(4):570-579.
32. Brealey D, Brand M, Hargreaves I, et al. Association between mitochondrial dysfunction and severity and outcome of septic shock. *Lancet.* 2002;360(9328):219-223.

33. Yarana C, Sripetchwandee J, Sanit J, Chattipakorn S, Chattipakorn N. Calcium-induced cardiac mitochondrial dysfunction is predominantly mediated by cyclosporine A-dependent mitochondrial permeability transition pore. *Arch Med Res.* 2012;43(5):333-338.
34. Arena G, Valente EM. PINK1 in the limelight: multiple functions of an eclectic protein in human health and disease. *J Pathol.* 2017;241(2):251-263.
35. Valente EM, Abou-Sleiman PM, Caputo V, et al. Hereditary early-onset Parkinson's disease caused by mutations in PINK1. *Science.* 2004;304(5674):1158-1160.
36. Billia F, Hauck L, Konecny F, Rao V, Shen J, Mak TW. PTEN-inducible kinase 1 (PINK1)/Park6 is indispensable for normal heart function. *Proc Natl Acad Sci U S A.* 2011;108(23):9572-9577.
37. Siddall HK, Yellon DM, Ong SB, et al. Loss of PINK1 increases the heart's vulnerability to ischemia-reperfusion injury. *PLoS One.* 2013;8(4):e62400.
38. Dagda RK, Pien I, Wang R, et al. Beyond the mitochondrion: cytosolic PINK1 remodels dendrites through protein kinase A. *J Neurochem.* 2014;128(6):864-877.
39. Okatsu K, Oka T, Iguchi M, et al. PINK1 autophosphorylation upon membrane potential dissipation is essential for Parkin recruitment to damaged mitochondria. *Nat Commun.* 2012;3:1016.
40. Rakovic A, Grunewald A, Kottwitz J, et al. Mutations in PINK1 and Parkin impair ubiquitination of Mitofusins in human fibroblasts. *PLoS One.* 2011;6(3):e16746.
41. Seibler P, Graziotto J, Jeong H, Simunovic F, Klein C, Krainc D. Mitochondrial Parkin recruitment is impaired in neurons derived from mutant PINK1 induced pluripotent stem cells. *J Neurosci.* 2011;31(16):5970-5976.
42. Lazarou M, Sliter DA, Kane LA, et al. The ubiquitin kinase PINK1 recruits autophagy receptors to induce mitophagy. *Nature.* 2015;524(7565):309-314.

Figures

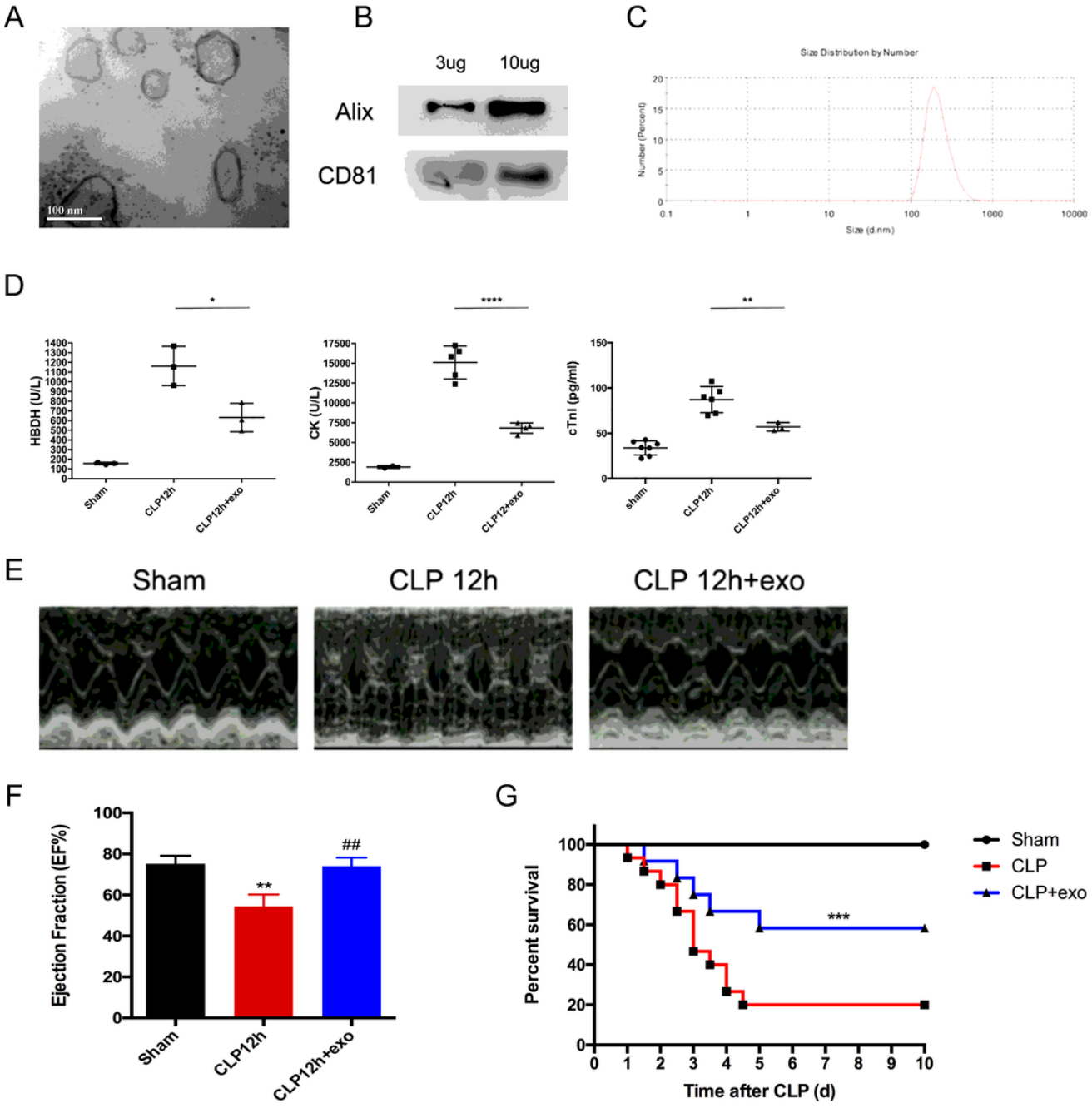

Figure 1

huMSCs-exo showed cardioprotective effects in septic mice. A-C: Characterizations of exosomes derived from huMSCs: A): electron micrographs of huMSCs exosomes, B): the size of huMSCs exosomes measured using a particle size analyzer, C): exosome markers detected by Western blot. D: Detection of myocardial injury serological markers HBDH, CK and cTnI; *p<0.05, **p<0.01, ****p<0.0001 when compared between mice 12 hr after CLP and the huMSCs-exo treatment group. E: Representative echocardiography of the sham, CLP 12 hr and CLP 12 hr+exo groups. F: Measurement of ejection fraction; **p<0.01 vs. sham group, ##p<0.01 vs. CLP 12 hr group. G: Survival in mice following huMSCs-exo treatment after CLP. Comparisons between groups were performed by Kaplan-Meier analysis followed by log-rank tests; ***p<0.001 vs. CLP group.

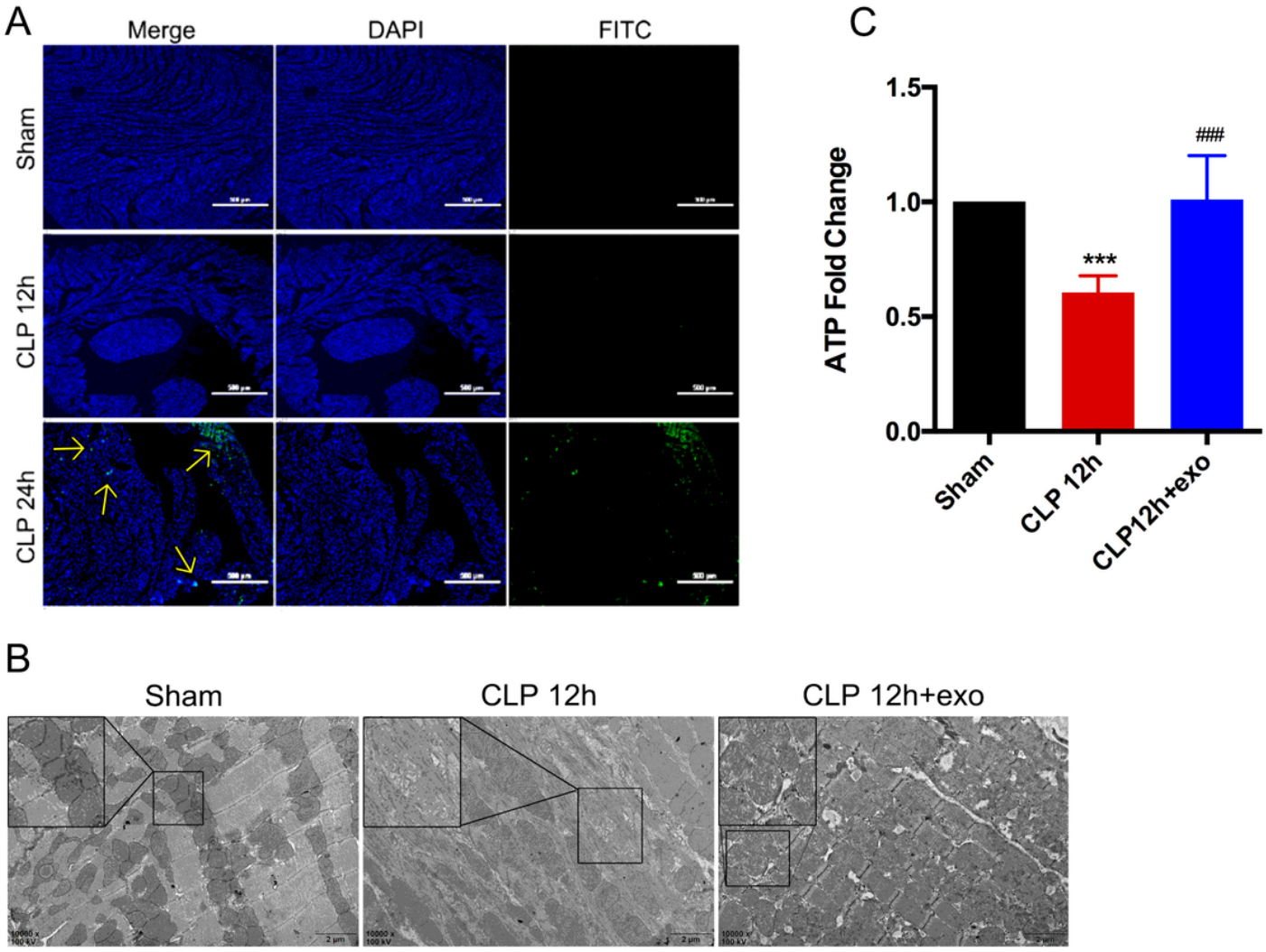

Figure 2

Sepsis-induced heart dysfunction is caused by mitochondrial injury, which is reversed by huMSCs-exo. A: Representative TUNEL staining for the detection of apoptotic cardiomyocytes (green dots indicated by arrows); nuclei were stained with DAPI (blue). B: After CLP for 12 hr and treatment with huMSCs-exo, the mitochondrial architecture was observed under transmission electron microscopy (TEM) and imaged at a 10000 × magnification (scale bars, 2 μm); the box in the image is a local magnification. C: The cardiomyocyte ATP content in mice 12 hr after the CLP and those with huMSCs-exo treatment was measured using a bioluminescent assay system; ***$p<0.001$ vs. sham group, ###$p<0.001$ vs. CLP 12 hr group.

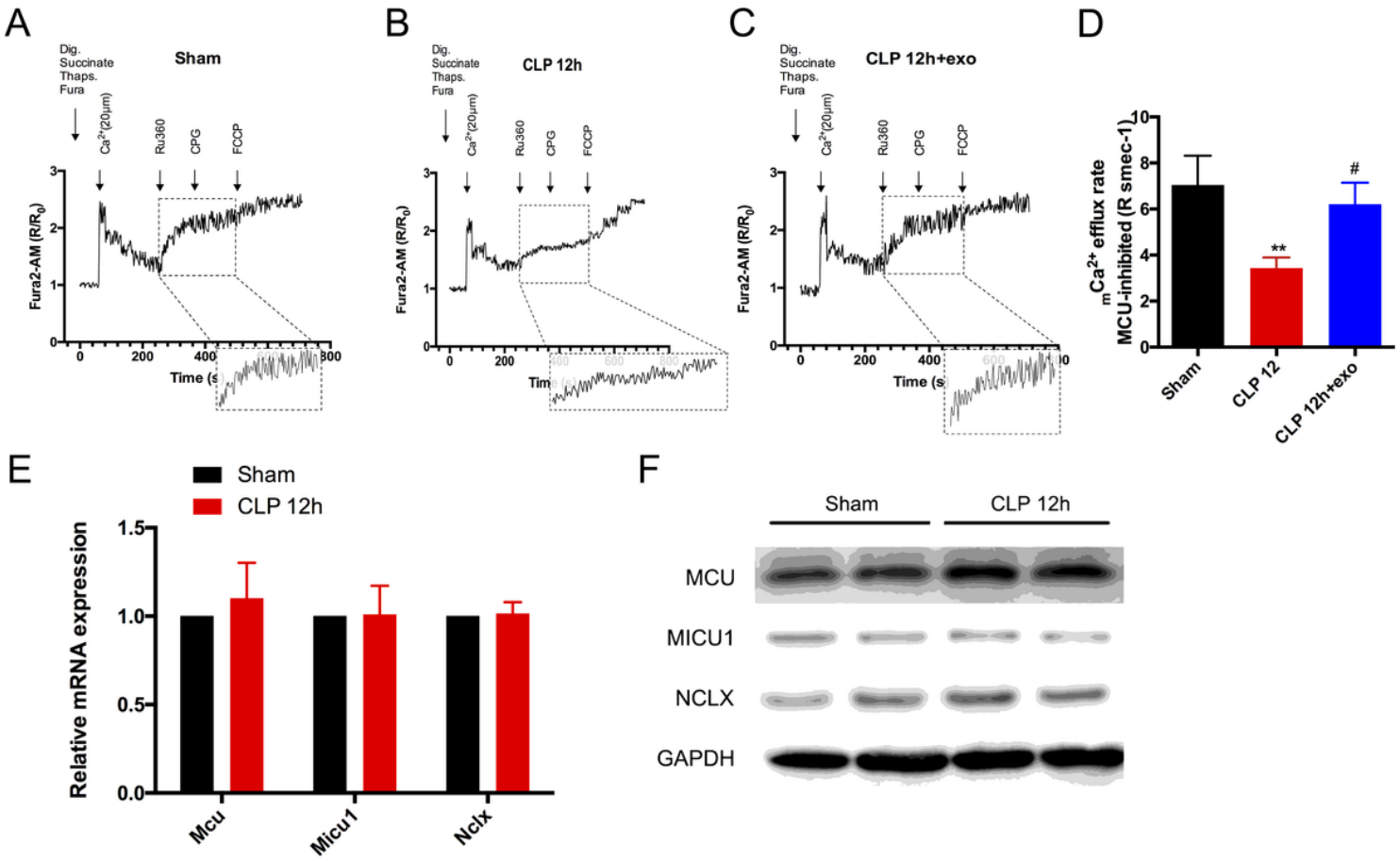

Figure 3

Assessment of cardiomyocyte mitochondrial Ca2+ (mCa2+) uptake, efflux and the corresponding regulator. A-C: mCa2+ uptake and efflux in isolated permeabilized ACMs; dig.: digitonin, thaps.: thapsigargin, Ru360: MCU inhibitor, CGP: NCLX inhibitor; the box shows a magnified mCa2+ efflux tracing (260 s-360 s); R indicates the ratio of the ratiometric reporter Fura-2 (340/380 nm excitation and 510 nm emission). R/R0 indicates the ratio at each time point over the ratio at time 0. D. mCa2+ efflux rate, n = 3 replicates per group; **p<0.01, #p<0.05. E. FQ-PCR detected the mRNA expression levels of Mcu, Micu1 and Nclx in the heart after CLP for 12 hr. F. Western blotting was used to detect MCU, MICU1 and NCLX expression in hearts 12 hr after CLP. GAPDH was used as a loading control.

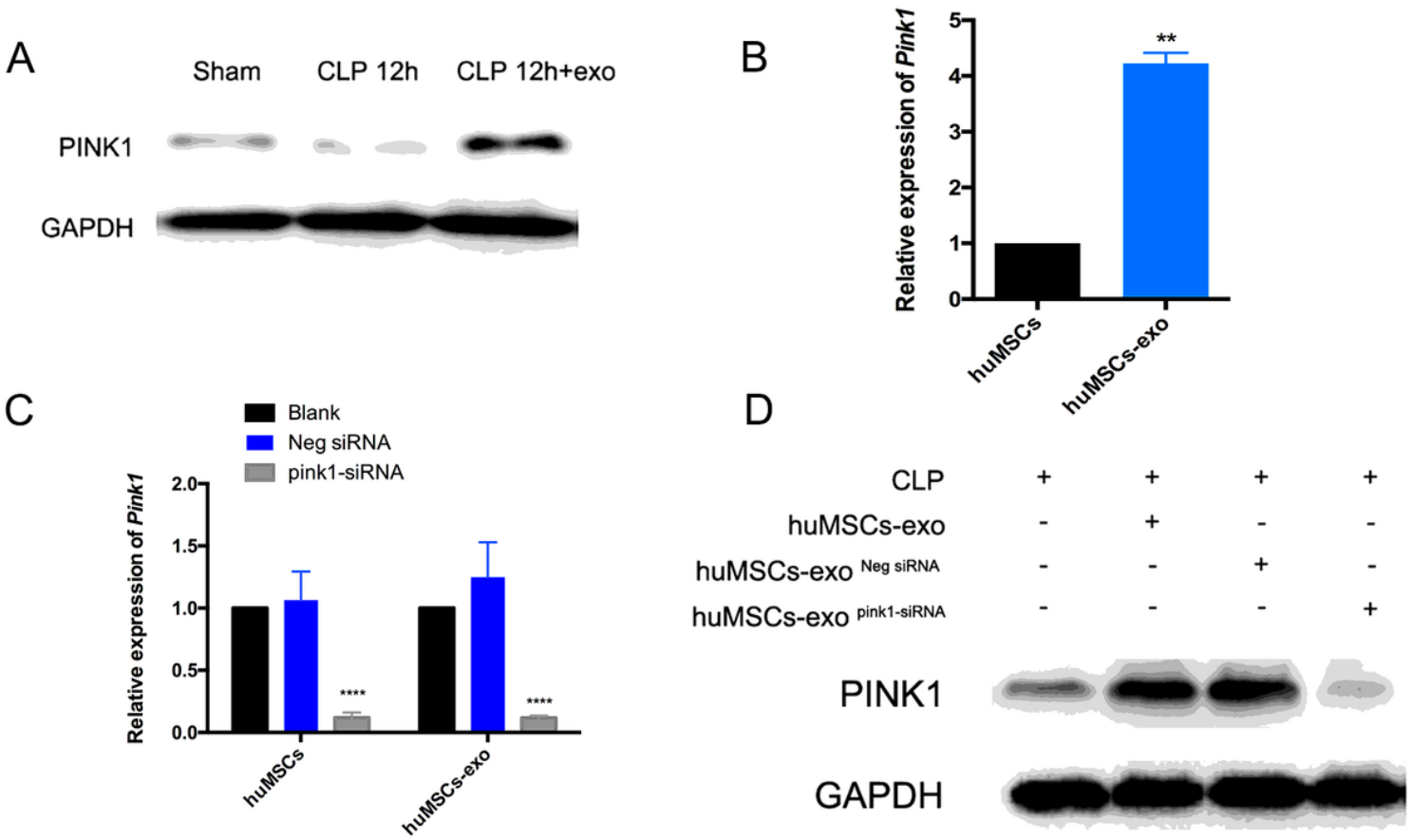

Figure 4

Sepsis decreased the expression of PINK1 in cardiomyocytes, and huMSCs-exo could transfer Pink1 mRNA into cardiomyocytes to increase PINK1 expression. A: Western blot detected PINK1 expression in hearts 12 hr after CLP and after treatment with huMSCs-exo; GAPDH was used as a loading control. B-C: The relative expression of Pink1 mRNA in huMSCs, huMSCs-exo (B) and in huMSCs, huMSCs-exo transfected with siRNA (C); **p<0.01 vs huMSCs group, ****p<0.0001 vs Neg siRNA group. D: Western blot analysis of PINK1 expression in the heart 12 hr after CLP and after treatment with huMSCs-exo or huMSCs-exo transfected with siRNA; GAPDH was used as a loading control.

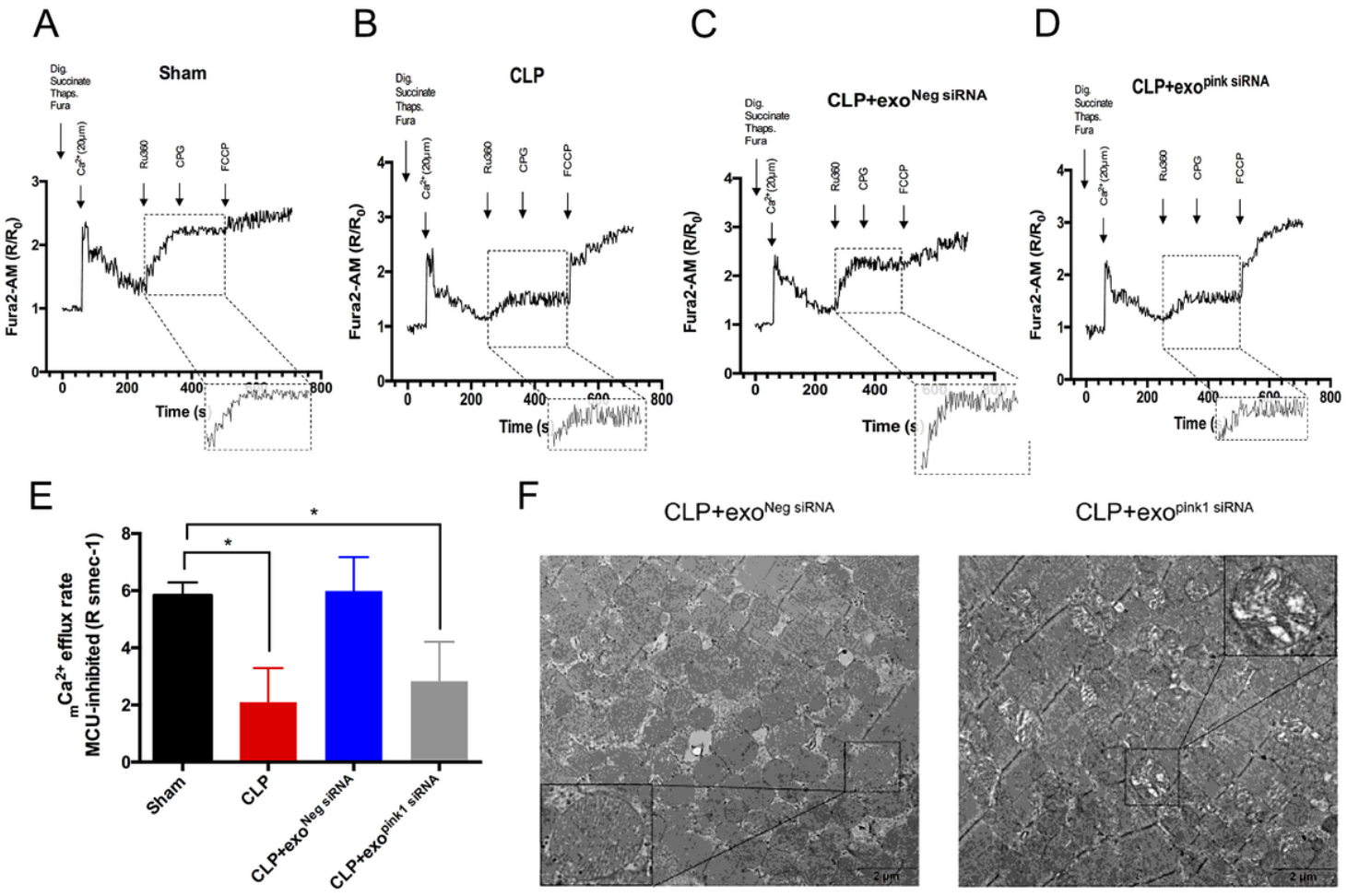

Figure 5

huMSCs-exo with inhibited Pink1 could not reverse mCa2+ efflux obstruction and mitochondrial damage induced by sepsis. A-D: mCa2+ uptake and efflux in isolated permeabilized ACMs; dig.: digitonin, thaps.: thapsigargin, Ru360: MCU inhibitor, CGP: NCLX inhibitor; the box shows a magnified mCa2+ efflux tracing (260 s-360 s); R indicates the ratio of the ratiometric reporter Fura-2 (340/380 nm excitation and 510 nm emission). R/R0 indicates the ratio at each time point over the ratio at time 0. E: mCa2+ efflux rate, n = 3 replicates per group, *p<0.05. F: Mitochondrial architecture observed with TEM after treatment with siRNA-transfected huMSCs-exo, imaged at a 10000 × magnification (scale bars, 2 μm), and the box in the image is a local magnification.

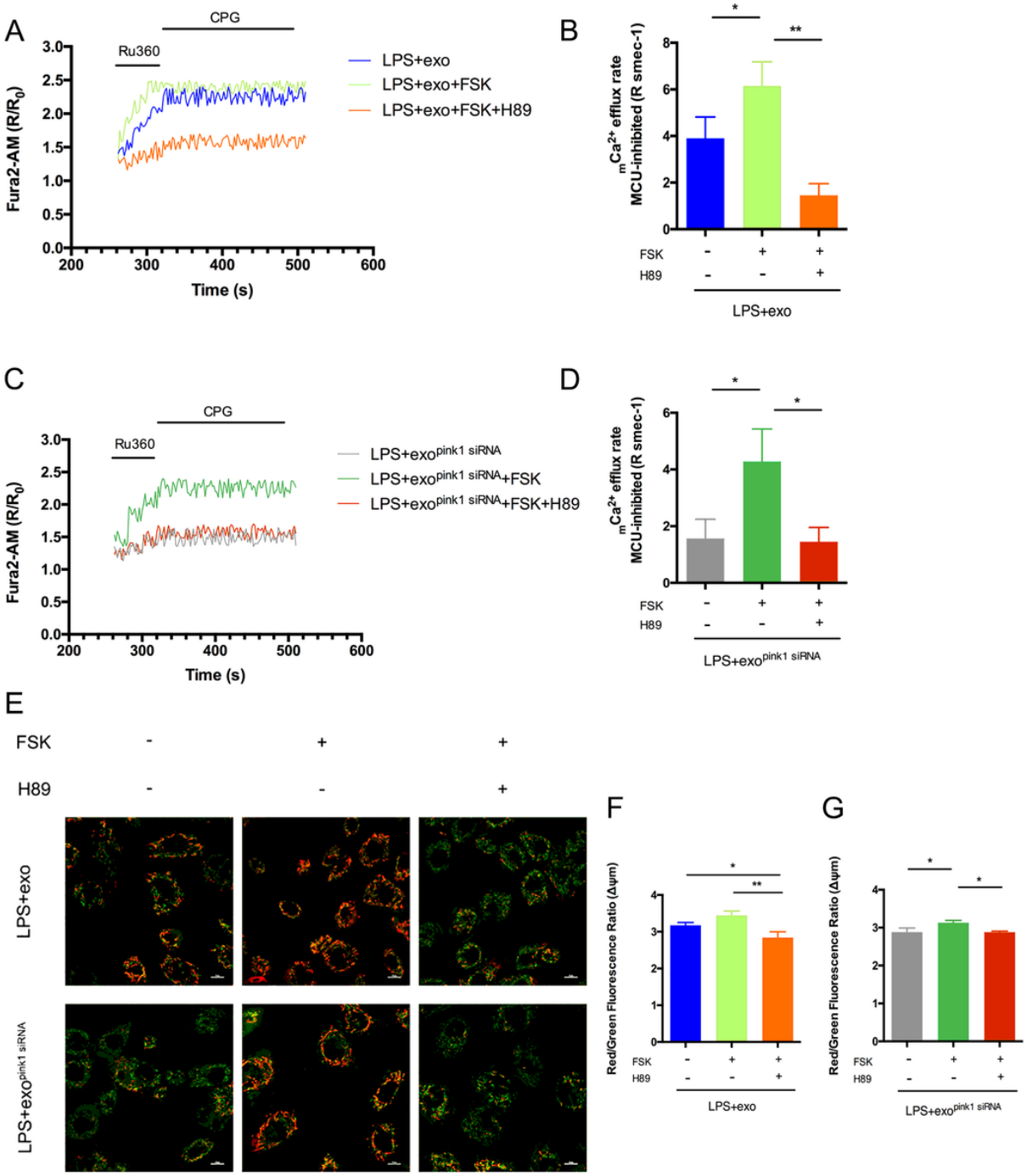

Figure 6

PINK1 transferred from huMSCs-exo regulated mCa2+ efflux by affecting PKA activity in cardiomyocytes. A: AC16 cells were treated with LPS and huMSCs-exo, and FSK or both FSK and H89 were added. After that, the mCa2+ efflux of cells was detected; Ru360: MCU inhibitor, CGP: NCLX inhibitor. B: Average mCa2+ efflux rates of Figure 6A, n = 3 replicates per group; *p<0.05, **p<0.01. C: AC16 cells were treated with LPS and Pink1-inhibited huMSCs-exo, after which FSK or both FSK and H89 were added. Subsequently, the mCa2+ efflux of cells was assessed; Ru360: MCU inhibitor, CGP: NCLX inhibitor. D: Average mCa2+ efflux rates of Figure 6C, n = 3 replicates per group; *p<0.05. E-G: Mitochondrial membrane potential analysis was measured using a fluorescence probe JC-1 assay system. The images were captured by confocal microscopy (E), and the ratio of red/green fluorescence represented the level of Δψm (F, G). The high ratio indicates a high mitochondrial membrane potential; *p<0.05, **p<0.01.